Journal of Hazardous Materials 198 (2011) 247–256

Contents lists available at SciVerse ScienceDirect

Journal of Hazardous Materials

journal homepage: www.elsevier.com/locate/jhazmat

Synthesis of novel inorganic–organic hybrid materials for simultaneous adsorption of metal ions and organic molecules in aqueous solution

Xinliang Jin, Yanfeng Li*, Cui Yu, Yingxia Ma, Liuqing Yang, Huaiyuan Hu

State Key Laboratory of Applied Organic Chemistry, College of Chemistry and Chemical Engineering, Institute of Biochemical Engineering & Environmental Technology, Lanzhou University, Lanzhou 730000, PR China

ARTICLE INFO

Article history:
Received 29 June 2011
Received in revised form
25 September 2011
Accepted 12 October 2011
Available online 18 October 2011

Keywords:
Hybrid materials
Amphiphilic
Pb(II)
Phenol
Adsorption

ABSTRACT

In this paper, atom transfer radical polymerization (ATRP) and radical grafting polymerization were combined to synthesize a novel amphiphilic hybrid material, meanwhile, the amphiphilic hybrid material was employed in the absorption of heavy metal and organic pollutants. After the formation of attapulgite (ATP) ATRP initiator, ATRP block copolymers of styrene (St) and divinylbenzene (DVB) were grafted from it as ATP-P(S-*b*-DVB). Then radical polymerization of acrylonitrile (AN) was carried out with pendent double bonds in the DVD units successfully, finally we got the inorganic–organic hybrid materials ATP-P(S-*b*-DVB-g-AN). A novel amphiphilic hybrid material ATP-P(S-*b*-DVB-*g*-AO) (ASDO) was obtained after transforming acrylonitrile (AN) units into acrylamide oxime (AO) as hydrophilic segment. The adsorption capacity of ASDO for Pb(II) could achieve 131.6 mg/g, and the maximum removal capacity of ASDO towards phenol was found to be 18.18 mg/g in the case of monolayer adsorption at 30 °C. The optimum pH was 5 for both lead and phenol adsorption. The adsorption kinetic suited pseudo-second-order equation and the equilibrium fitted the Freundlich model very well under optimal conditions. At the same time FT-IR, TEM and TGA were also used to study its structure and property.

1. Introduction

As large numbers of heavy metal and organic pollutants were discharged into water environment from plating plants, mining, metal finishing, dyeing factories and several other industrial factories [1–3], so that their decontamination has become a major research topic for the wastewater treatments [4,5]. Heavy metal is harmful to human beings especially lead poisoning can cause hypertension, behavioral changes, learning disabilities, reading problems, development defects and language difficulties [6]. Particular attention is given to remove lead from wastewater rather urgently. Compared with traditional processes, lead removal by special adsorbent materials may have some advantages, such as convenient, economy, repeatable and green. Recent studies of the special adsorbent materials focus on activated carbon [7–9], mineral adsorbents [10,11], biosorbents [12–14], composites [15,16] and wide-spread and cheap natural materials or reused waste [17–22].

Phenols are classified as priority pollutants owing to their toxicity to organisms even at low concentrations [23]. In view of the high toxicity, wide prevalence and poor biodegradability of phenols [24] and the US Environmental Protection Agency (EPA) regulations call for lowering phenol content in the wastewater to less than 1 mg/l [25], it is necessary to remove them from wastewaters before discharge into water bodies. Treatments of phenolic wastewater include extraction with organic solvents [26], separation with membranes [27] and adsorption in porous [28] or functional [29,30] solids. The last process is the most widely used due to its relatively simple implementation and low operation cost. In recent years, there have been many investigations, with the aim of finding effective adsorbents for the treatment of phenolic aqueous wastes. Thus, the most used adsorbents are activated carbon [31,32], silica [33], montmorillonite [34], organophilic clays [35,36] and others.

In our previous works, series of novel adsorbents, chelating resins [37–40], polysulfone capsules [41–43], polyvinyl alcohol (PVA) [44,45] were successfully synthesized and employed in the removal of heavy metal and organic toxic pollutants in water environment. Recent studies have shown that more and more novel adsorption materials have been developed [46,47], however, few researches on new materials, which are synthesized to adsorb heavy metal and organic wastes at the same time, have been reported.

Amphiphilic copolymers, involving drug carriers for targeted drug delivery and sensitive to environment materials, etc., have

* Corresponding author. Fax: +86 9318912113.
E-mail address: liyf@lzu.edu.cn (Y. Li).

0304-3894/$ – see front matter © 2011 Elsevier B.V. All rights reserved.
doi:10.1016/j.jhazmat.2011.10.040

recently attracted much attentions in a broad range of fields [48,49], and the grafting and block copolymerization will be useful methods for getting functional copolymers [50]. Especially, atom transfer radical polymerization (ATRP) could not only offer a new kind of synthesis way for well-defined macromolecular architecture such as amphiphilic random, and block copolymers [51,52], but has prepared a wide range of new type copolymers [53,54], e.g., many excellent works on polymer brushes on the surfaces of zeolite [55] and layered silicate [56] have been reported.

In this work, ATRP and radical grafting polymerization were introduced in order to synthesize a novel amphiphilic hybrid material. At first, a novel block copolymer, P(S-*b*-DVB-*g*-AN), was grafted from ATRP initiator – the modified attapulgite (ATP). ATRP of styrene (St) and divinylbenzene (DVB) took place from the initiator sequentially, following the radical grafting polymerization of acrylonitrile (AN) was carried out with the pendent double bonds in the DVB units, successively. After the AN units in the resulting block copolymers were converted into acrylamide oxime (AO) in the presence of nitrile group and hydroxylammonium chloride, a novel amphiphilic hybrid material ATP-P(S-*b*-DVB-*g*-AO) was obtained, which is abbreviated into ASDO. FT-IR, TEM, and TGA methods were used to analyze new structures of the resulting materials, and the adsorption properties of the resulting ASDO adsorbent for Pb(II) and phenol in aqueous solution were investigated at the same time.

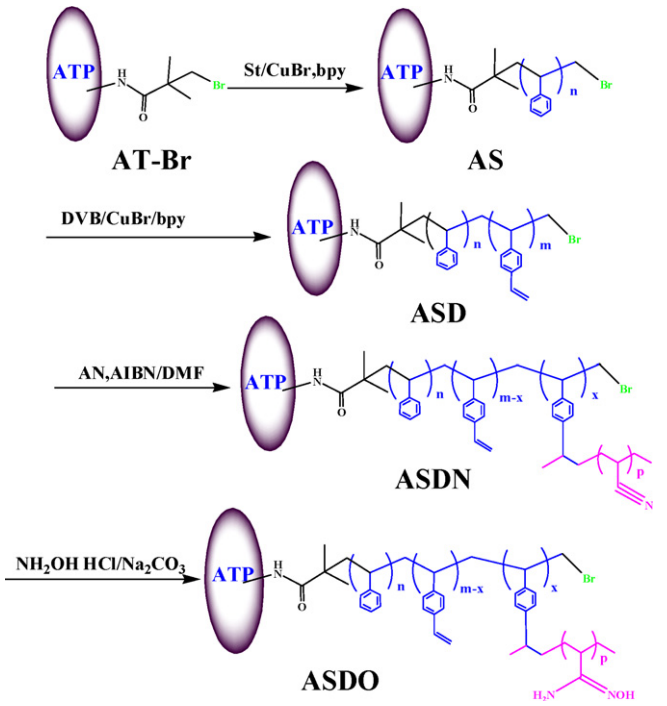

Fig. 1. Scheme of the preparation procedure of ASDO.

2. Experimental

2.1. Materials

Attapulgite (ATP) with the average diameter of 325 mesh, was provided by Gansu ATP Co. Ltd., Gansu, China. γ-Aminopropyl triethoxy silane (KH-550) was supported by Wu Han University. 2-Bromoisobutyryl bromide (BB)(98%, Aldrich) was used as received. Styrene (St) (≥99%, Sinopharm Chemical Regent Co. Ltd.) was purified by extracting with 5% sodium hydroxide aqueous solution, followed by washing with water and dried with anhydrous sodium sulfate overnight, finally distillated under vacuum. Divinylbenzene (80%, DVB) (Aldrich) was purified by passing through a column of activated basic alumina and purging with high-purity nitrogen for 1 h prior to use. CuBr (≥98.5%, Shanghai Chemical Reagent Co. Ltd.) was dissolved in acetic acid, washed with ethanol and ether in turn then dried under vacuum. Toluene (99.5%, Tianjin Guangfu Fine Chemical Research Institute) was distilled over CaH_2. 2,2′-Bipyridyl (bpy) (≥99.5%, Shanghai Chemical Reagent Co. Ltd.), and $CuBr_2$ (≥98.5%, Shanghai Chemical Reagent Co. Ltd.) were used as received. All other chemicals of analytical grade were provided by Tianjin Guangfu Fine Chemical Research Institute and were used as received without any further purification.

2.2. Synthesis of ASDO

Fig. 1 shows the synthesis process of ASDO. The process is divided into three stages, introducing initiator onto surface of ATP, synthesis of hydrophobic block inorganic–organic hybrid materials, and synthesis of amphiphilic inorganic–organic hybrid materials. Fig. 2 shows the proposed schematic diagram of the preparation procedure of ASDO. Hydrophobic polymer segments P(S-*b*-DVB) are grafted from ATP which are used to adsorb organic molecules; divinylbenzene (DVB) was introduced to build hyperbranched hydrophobic structure and to import reserved double bonds for the next radical polymerization; poly(acrylamide oximes) (PAOs) introduced into the outermost layer of the hybrid materials by free radical copolymerization have a strong metal ion chelation capacity.

2.2.1. Synthesis of ATP-Br

2.2.1.1. Preparation of KH-550-modified ATP nanocomposites. The coupling reagent KH-550 was used to introduce amino groups onto the ATP surface before the graft polymerization initiator was surface-initiated. Typically, 2.00 g of ATP was dispersed in 60 ml of ethanol by sonication for about 0.5 h, then 6.0 ml of $NH_3{\cdot}H_2O$ was

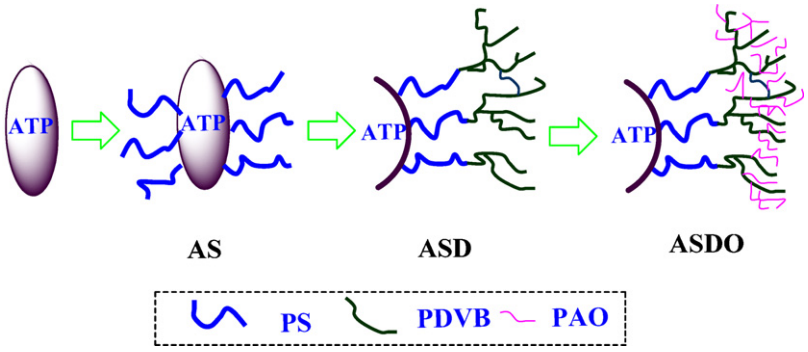

Fig. 2. Proposed schematic diagram of the preparation procedure of ASDO.

added and sonicated to homogenize for 10 min. Under continuous mechanical stirring, 4.0 ml of KH-550 was added to the reaction mixture. The reaction was allowed to proceed at 50 °C for 8 h under continuous stirring under N_2 atmosphere. After that, the resultant products were separated by centrifugation and were washed with ethanol and distilled water until neutral. The KH-550-modified ATP was dried in a desiccator at 50 °C overnight.

1.00 g of dried KH-550-modified ATP was dispersed in 60 ml of dried THF by sonication for about 0.5 h in a round bottom flask, next was cooled in an ice-water bath for 2 h with a stir bar. Then 2.00 ml of triethylamine was added drop wise. The mixture was stirred for another 30 min in the ice-water bath, and then 2.00 ml of 2-bromoisobutyryl bromide was added. The amidation reaction was conducted at 0 °C for 4 h, followed by another 20 at room temperature. After this, a gray powder, separated from the solvent by centrifugation, was fully washed with water, and ethanol to remove any physically adsorbed species. The sample was dried at 40 °C overnight before further characterization.

2.2.2. Synthesis of hydrophobic block inorganic–organic hybrid materials

Synthesis of ATP-PS (AS) [57]**.** A 50 ml two-necked flask with a magnetic bar was evacuated and purged with pure nitrogen three times, 0.50 g of ATP-Br, 4.5 ml of toluene, and 9 ml of St was then added, and stirring was commenced. Under nitrogen atmosphere, 0.111 g of CuBr and 0.162 ml of PMDETA were then added and deoxygenated by three consecutive freeze–pump–thaw cycles. The tube was sealed under a nitrogen atmosphere and stirring for 30 min at room temperature and then placed in a thermostatic oil bath stirring for 24 h at 110 °C. The polymerization was stopped by cooling the mixture in the air and exposure to oxygen. After some time, the viscous mixture was then diluted with THF and the copolymer-grafted ATP nanoparticles were separated by centrifugation. Several washings of the AS with THF were done to remove ungrafted PS. The product was isolated by precipitation in a large excess of methanol, washed 2–3 times with pure methanol and distilled water respectively, which removed virtually all the remaining Cu-salts. For use in further ATRP, ATP-PS was thoroughly extracted in a Soxhlet extractor for 48 h with toluene, dried in vacuum, and dried in a desiccator at 50 °C.

Synthesis of ATP-P(S-*b*-DVB) (ASD). Polymerization procedure [58] was as followed. 0.25 g of ATP-PS, 5.00 ml of toluene, and 5.00 ml of DVB was added to a round bottom flask with a three-way stopcock connected to either a nitrogen line or a vacuum pump. Oxygen was removed by repeated vacuum–nitrogen cycles and then 0.0444 g of CuBr and 0.0941 g of bpy were added. After the flask was cycled between vacuum and nitrogen (×6 times) the reaction was stirred for 0.5 h at room temperature and then the flask was immersed in a preheated (90 °C) oil bath. After polymerization under stirring at the chosen reaction temperature (typically 90 °C) for 12 h, the powder was separated by centrifugation and washed as the step above. The hydrophobic modified ATP was dried under reduced pressure at 50 °C overnight.

2.2.3. Synthesis of amphiphilic inorganic–organic hybrid materials

After the nano-hybrid materials was modified with PDVB, a lot of –C=C suspended were left to react with acrylonitrile (AN) by free radical polymerization [58].

Synthesis of ATP-P(S-*b*-DVB-*g*-AN) (ASDN). 0.5 g of ATP-P(S-*b*-DVB) and 5.0 g of AN were added into 50 ml of DMF and sparged with a slow stream of nitrogen for 0.5 h while stirring. Then 0.25 g of azo-bis-isobutryonitrile (AIBN) was added and the flask was placed in an oil bath at 80 °C under nitrogen for 8 h. After that, the products were separated by centrifugation and were thoroughly washed with DMF, distilled water, and ethanol, then dried at room temperature under vacuum for 24 h.

Synthesis of ATP-P(S-*b*-DVB-*g*-AO) (ASDO). 0.50 g of $NH_2OH{\cdot}HCl$, 4.80 g of Na_2CO_3, 8.1 ml deionized water, and 50 ml of ethanol were added into a reactor equipped with a magnetic stirrer and a reflux condensator, the mixture was stirred for 0.5 h. After that, 0.50 g of ASDN nanocomposites was added to this mixture. The reaction was performed in two steps, 4 h at 40 °C and then 10 h at 85 °C under stirring. The modified hybrid materials were washed thoroughly with a large amount of distilled water then extracted by ethanol for 12 h, dried at 50 °C under vacuum for 12 h.

2.3. Adsorption experiments

All the adsorption experiments were carried out at adsorbent dosages of 2 g/l by shaking in a shaking thermostatic bath (SHZ-B, China) at 140 rpm at 25 °C for a given time. After adsorption, the solid and liquid phases were separated by centrifugation. Pb(II) concentrations in the solution samples were determined by atomic absorption spectrophotometer (AAS) while phenol concentrations were analyzed by a PERSEE TU-1810 UV–vis spectrophotometer at a wavelength of 271 nm. The pH of solutions was determined using a HANNA pH meter.

Pb(II) adsorption isotherms and the effects of the initial concentration were studied in the range of 50–645 ppm. The effects of pH were studied in the range of 1.0–6.0, with 0.1 mol/l HNO_3 and NaOH used as pH controls. The effects of contact time on adsorption were determined in the range of 0–48 h.

Phenol adsorption isotherms and the effects of the initial concentration were studied in the range of 50–500 ppm. The effects of pH were studied in the range of 3.0–13.0, with 0.1 mol/l HCl and NaOH used as pH controls. Contact time on adsorption was determined in the range of 0–24 h.

2.4. Characterization

FT-IR spectra were obtained for ATP, surface-initiated ATP-Br, AS, ASD, ASDN, and ASDO with a Nicolet Magna-IR 550 spectrophotometer between 4000 and 450 cm^{-1}.

Transmission electron microscopies (TEM) were studied with a Tecnai-G2-F30 Field Emission Transmission Electron Microscope.

TGA was conducted with a TA Instruments STA449, and experiments were carried out on approximately 10 mg of samples in flowing air (flowing rate = 100 cm^3/min) at a heating rate of 20 °C/min.

3. Results and discussion

3.1. Surface modification reactions

The pathway of preparing ASDO can be outlined as in Fig. 1. The ATRP initiator was first immobilized on the surfaces of the ATP through the interaction with the $–NH_2$ groups; then the polymerization of St started from the surface-initiated ATP, the hyper branched chains of PDVB grew from the (ATP-PS)-Br by polymerizing additional DVB molecules from the (ATP-PS)-Br; PAN chains were connected with the system from left double bonds in PDVB by free radical polymerization.

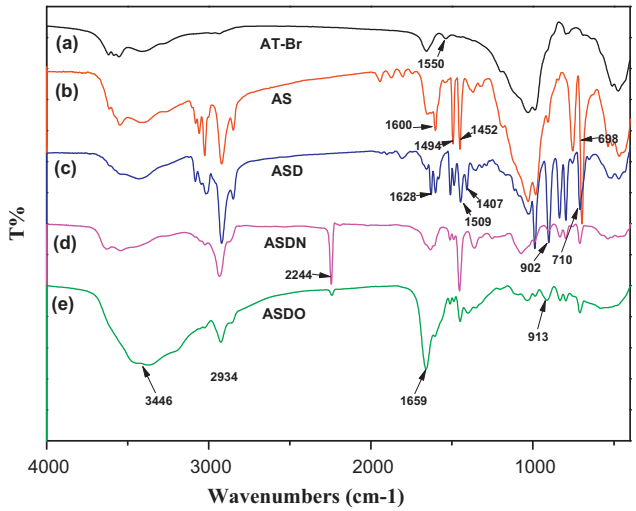

Fig. 3. FT-IR spectra of (a) ATP-Br, (b) AS, (c)ASD, (d) ASDN and (e) ASDO.

Table 1
Characteristics of FT-IR transmission bands of ATP-Br, AS, ASD, ASDN and ASDO.

Sample	Band (cm^{-1})	Assignment
ATP-Br	1550	–CO–NH–
AS	2000–1600	Characteristic peak of benzene ring
	1494, 1452, 760, 698	Monosubstituted benzene ring peak
ASD	1628, 1407, 990, 902	–C=C
ASDN	2244	–C≡N
	1659	υ-C=N
ASDO	913	υ-N–O
	3446	υ-OH

3.1.1. FT-IR spectroscopic analyses

Fig. 3 shows the FT-IR spectra of surface-initiated ATP (ATP-Br), ATP-PS (AS), ATP-PS-PDVB (ASD), ATP-PS-PDVB-PAN (ASDN), and ATP-PS-PDVB-PAO (ASDO), meanwhile, the characteristic peaks of each product properly attributed are shown in Table 1. It can be seen from Fig. 3 and Table 1 that the important features peaks of every step product have emerged in the spectrum, which suggests that the synthetic material is the target amphiphilic hybrid material.

3.1.2. TGA

Fig. 4 shows the TGA result of ASDO, which began to decompose at 290.21 °C, while AS began to decompose at 397.14 °C. AS and ASDO structures both containing polystyrene structure, so a similar weight loss trend appeared in the vicinity of 450–460 °C.

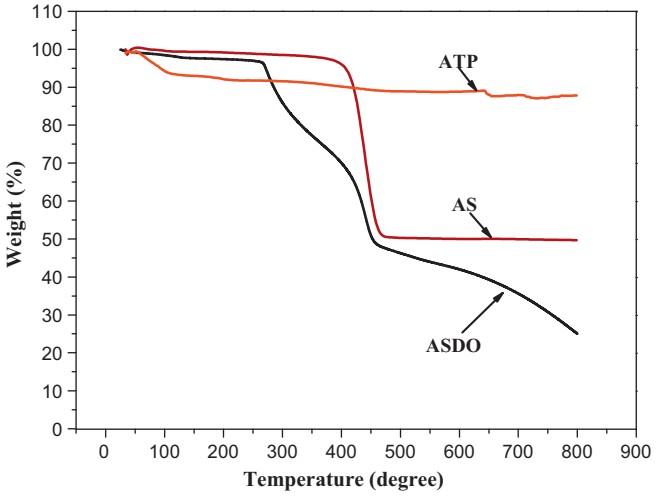

Fig. 4. TGA of (a) ATP, (b) AS and (c) ASDO.

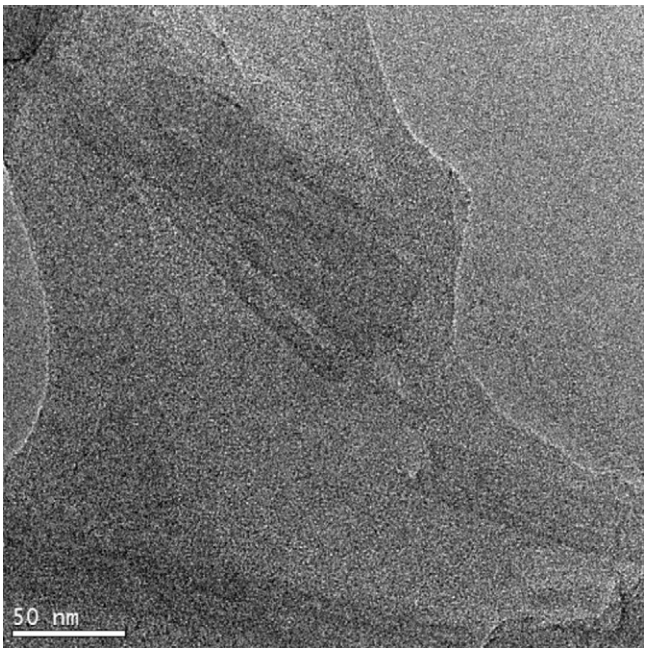

Fig. 5. TEM image of ASDO sample.

3.1.3. TEM analysis

TEM micrograph of ASDO is shown in Fig. 5. It is evident from the micrograph that negative charges take place at the surface of the ATP needles. It demonstrates that ATP-needles with a diameter of about 50 nm were wrapped by a large number of polymers.

3.2. Sorption studies

3.2.1. Adsorption of Pb(II) ions and phenol

3.2.1.1. Effect of solution pH. The effect of Pb(II) solution pH (1.0–6.0) on Pb(II) sorption onto the adsorbent material has been illustrated in Fig. 6a. Both the sorption capacity and the adsorptivity of Pb(II) increased significantly with a pH rise from 1.0 to 5.0 but decreased slightly with a further pH rise from 5.0 to 6.04. As pH is lower, the amino groups of amidoxime groups would lose the complex ability towards Pb(II) ions due to protonation [59], leading to the low adsorption ability of ASDO for Pb(II) ions. Along with the increase of pH value, the protonation degree of the amino groups of amidoxime groups would be weakened, and the coordination and chelating ability of these amino groups towards Pb(II) ions would be strengthened. In addition, here the dissociation degree of oxime hydroxyl groups would increase, and negative oxygen-ion of oxime hydroxyl groups would be produced, resulting in the electrostatic interaction between ASDO and Pb(II) ions. It is well established from speciation study of single lead species that in an aqueous solution of $Pb(NO_3)_2$, the formation of solid $Pb(OH)_2$ starts at pH 6.3 [60], and the surfaces of ASDO would be covered with the hydrolysis product. This would badly affect the adsorption property of the solid adsorbent [61] and lead to the decline of the adsorption capacity.

The effect of phenol solution pH 3.0–13.0 on phenol sorption onto the hybrid material has been illustrated in Fig. 6b and it can be found from Fig. 6b that the adsorption capacity gets up to a maximum as pH 5. The above facts reflect the interaction mechanism between ASDO and phenol, and it can be explained as follows. The amidoxime group has amphiprotic property [62], so the amidoxime groups of the grafted PAO will exhibit this property. At lower pH,

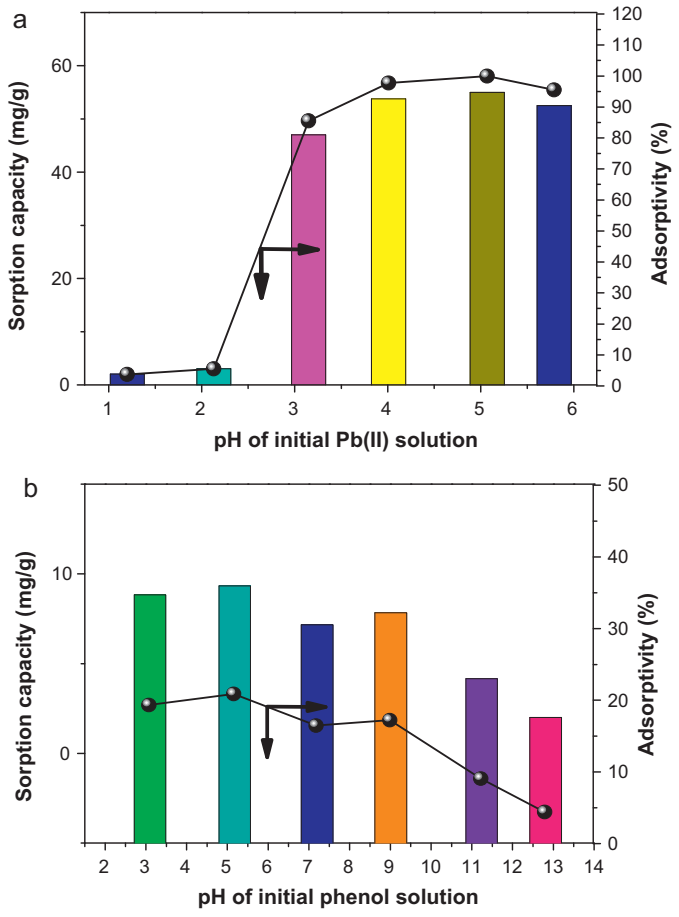

Fig. 6. Effect of pH on the adsorption of ASDO for (a) Pb(II) and (b) phenol.

the basic amino groups of amidoxime groups of ASDO will be highly protonized, displaying the cationic character, whereas at higher pH, the acidic hydroxyl groups of oxime groups will dissociate, exhibiting the anionic character. However, the p*K*a of phenol is 9.95 and typically the aqueous solution of phenol bears negative charges [63,64]. As pH is lower, the amino groups of amidoxime groups will enhance the attraction ability towards phenol due to protonation, but the degree of ionization of phenol will be inhibited, leading to the highest adsorption ability of ASDO for phenol when pH is 5. Along with the increase of pH value, the protonation degree of the amino groups of amidoxime groups will be weakened, and the dissociation degree of oxime hydroxyl groups will increase, and negative oxygen-ion of oxime hydroxyl groups will be produced, resulting in the electrostatic repulsion between ASDO and phenol.

3.2.1.2. Effect of sorption time and sorption kinetics. The relationship between reaction time and sorption amounts at the different initial Pb(II) concentrations is presented in Fig. 7a. The Pb(II) adsorbability on the adsorbent rises nonlinearly with increasing the sorption time. The sorption process can clearly be divided into two steps, an initial rapid step and a subsequent slow step. The sorption of Pb(II) ion onto ASDO is very rapid during the initial 3.67 h, for which the sorption capacity and adsorptivity reach up to 20.50 mg/g and 87.35% when the initial concentration is 23.46 mg/l, respectively, that are 99.96% of the sorption capacity and adsorptivity for 48 h. The initial rapid step of Pb(II) sorption may be attributed to the physical and surface reactive sorption due to a facilely immediate interaction between Pb(II) and the reactive groups (i.e. $-NH_2$, –OH and –C=N) on the surface of the adsorbent [65]. However, the subsequent slow step was attributable to the reactive sorption to the

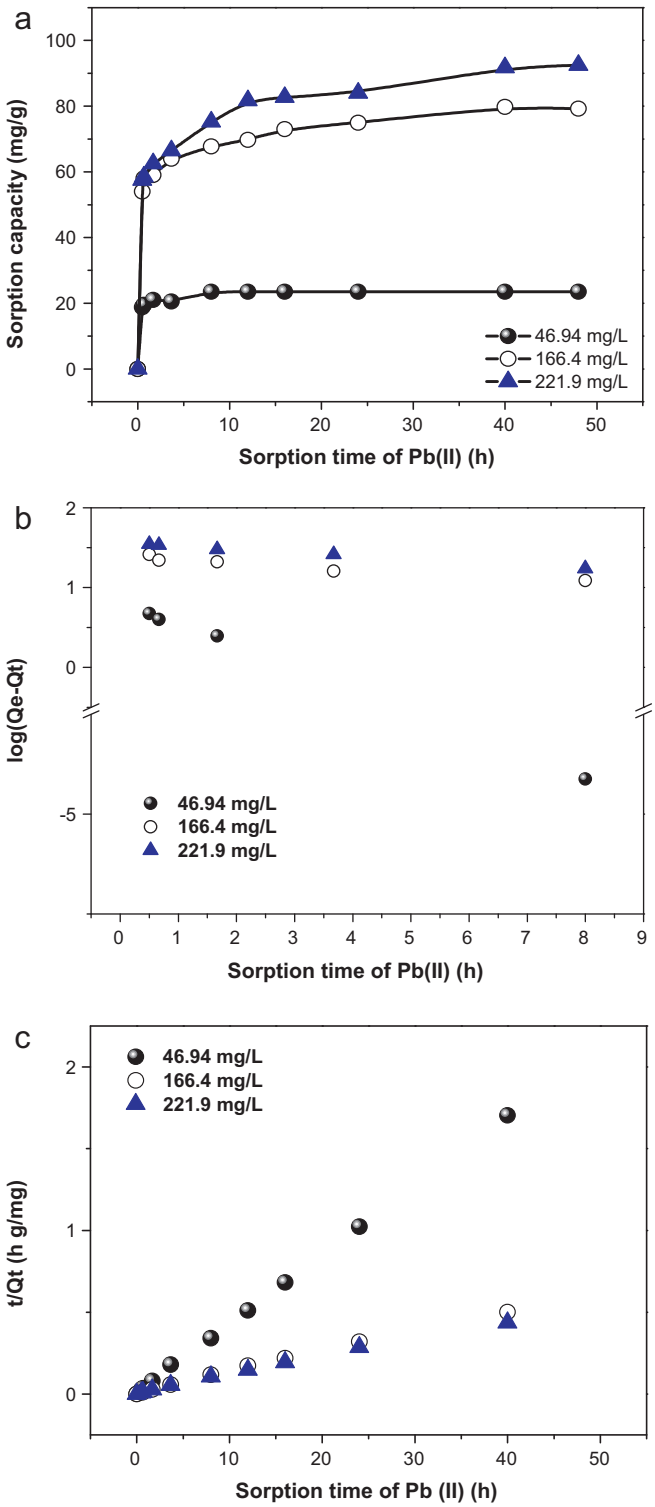

Fig. 7. Adsorption kinetics of ASDO for Pb(II): (a) effect of shaking time on adsorption of ASDO, (b) pseudo-first-order and (c) pseudo-second-order.

inner of the polymer chain segments, besides the Pb(II) adhere on the surface of the nano-adsorbent would further hamper the diffusion of Pb(II), resulting in a rather long time to reach the equilibrium sorption [66].

The adsorption kinetics that describes the solute uptake rate governing the contact time of the sorption reaction is one of the important characteristics that define the efficiency of sorption. The pseudo-first-order and pseudo-second-order kinetic equations

Table 2
Parameters of kinetics model for the adsorption of Pb(II) on ASDO with different initial concentrations.

C_0 (mg/l)	Pseudo-first-order			Pseudo-second-order		
	Q_{e1} (mg/g)	K_1 (h^{-1})	R_1^2	Q_{e2} (mg/g)	K_2 (g/mg h)	R_2^2
46.94	17.67	1.731	0.9897	23.58	0.2397	0.9999
166.4	24.58	0.0919	0.9350	80.65	0.0128	0.9986
221.9	36.07	0.0921	0.9960	93.46	0.0084	0.9976

were employed to analyze the sorption kinetics of Pb(II) ions onto the beads. Fig. 7b and c shows the curves of t/Q_t versus t and $\log(Q_e - Q_t)$ versus t based on the experiment data. From the corresponding parameters summarized in Table 2, it is observed that the kinetic behavior of Pb(II) sorption onto the adsorbent is more appropriately described by the pseudo-second-order model because of a much higher correlation coefficient. The pseudo-second-order model was developed based on the assumption that the determining rate step might be chemisorption promoted by covalent forces through the electron exchange or valence forces through electrons sharing between sorbent and sorbate [37], indicating that the behavior of Pb(II) sorption on ASDO was in agreement with chemical adsorption.

Fig. 8 represents the adsorption kinetics curves of the functional particles ASDO towards phenol. It can be seen from Fig. 8a that the adsorption of ASDO can reach equilibrium during 6 h. These results indicated that the adsorption process can be considered very fast because of large amount of phenol attached to ASDO within the first 2 h of adsorption. After a rapid sorption, the phenol sorption rates declined slowly and the equilibriums were reached at about 6 h. The kinetics data are plotted as the linear form of the models (Fig. 8), and the resultant parameters are given in Table 3. As can be seen from Table 1, the coefficients (R_1^2) for pseudo-first-order kinetic model are between 0.8868 and 0.9609 and the correlation coefficients (R_2^2) for pseudo-second kinetic model are between 0.9988 and 1.0000. These results show that phenol adsorption system of ASDO obeys the pseudo-second-order kinetic model.

3.2.1.3. Effect of initial concentration and sorption isotherm. Adsorption isotherm data have been described by the Langmuir adsorption isotherm and Freundlich equations.

Langmuir equation:

$$\frac{C_e}{Q_e} = \frac{1}{K_L Q_{max}} + \frac{C_e}{Q_{max}}$$

Freundlich equation:

$$\ln Q_e = \ln K + \frac{1}{n} \ln C_e$$

where C_e (mg/l) is the concentration of the phenol solution at equilibrium, Q_e (mg/g) is the amount of sorption at equilibrium. In Langmuir equation, Q_{max} is the maximum sorption capacity and K_L is Langmuir constant. In Freundlich equation, K and $1/n$ are empirical constants.

The relationship between the initial Pb(II) ion concentration and the adsorption capacities of ASDO for Pb(II) was studied. As shown in Fig. 9a, the adsorption capacities of ASDO for Pb(II) were positively correlated with the initial Pb(II) ion concentration because the adsorption process was highly concentration dependent. The Pb(II) adsorbance rises significantly with an increase in Pb(II) concentration, whereas the adsorptivity declines. When the initial Pb(II) ion concentration was increased from 50 mg/l up to 645 mg/l, the adsorption capacity increased from 24.99 mg/g to 131.7 mg/g. The adsorptivity could achieve in this study is 99.8% at the initial

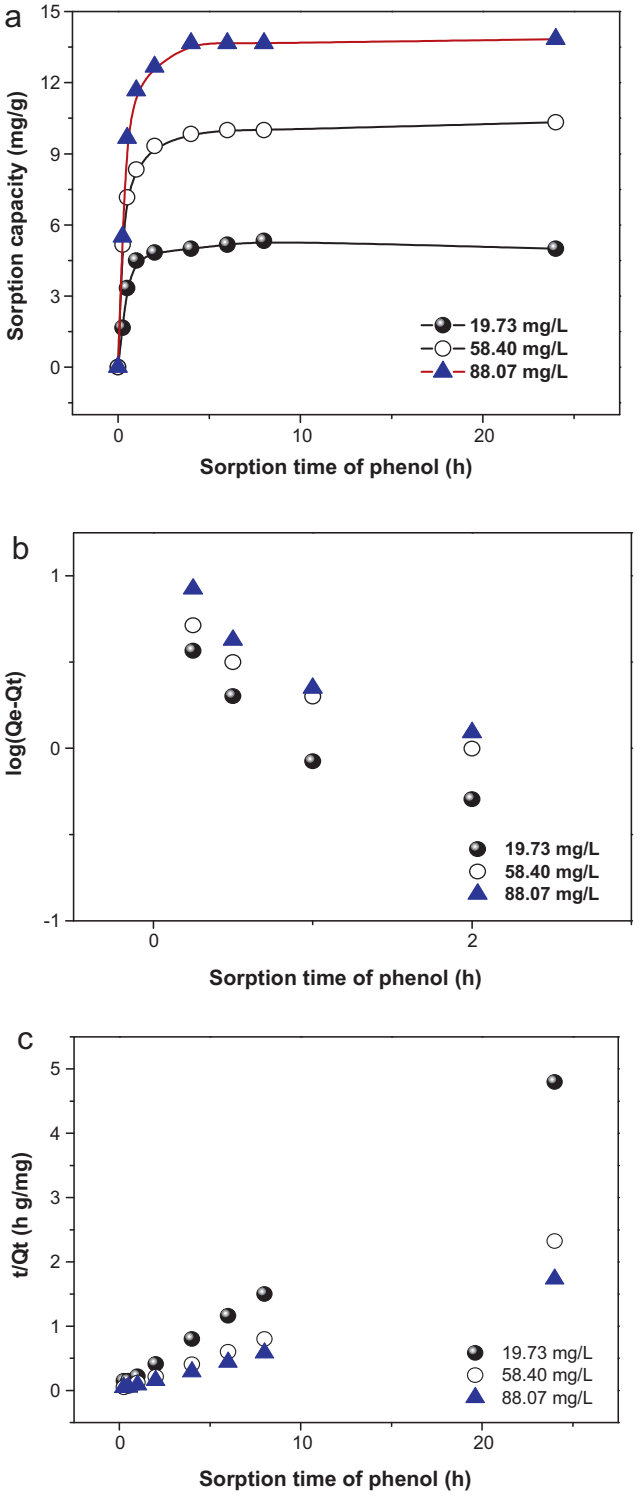

Fig. 8. Adsorption kinetics of ASDO for phenol: (a) effect of shaking time on adsorption of ASDO, (b) pseudo-first-order and (c) pseudo-second-order.

Table 3
Parameters of kinetics model for the adsorption of phenol on ASDO with different initial concentrations.

C_0 (mg/l)	Pseudo-first-order			Pseudo-second-order		
	Q_{e1} (mg/g)	K_1 (h^{-1})	R_1^2	Q_{e2} (mg/g)	K_2 (g/mg h)	R_2^2
19.73	3.65	1.076	0.8868	5.07	1.792	0.9988
58.40	5.48	0.8866	0.9609	10.43	0.3754	1.0000
88.07	8.14	1.038	0.9020	13.99	0.3386	0.9999

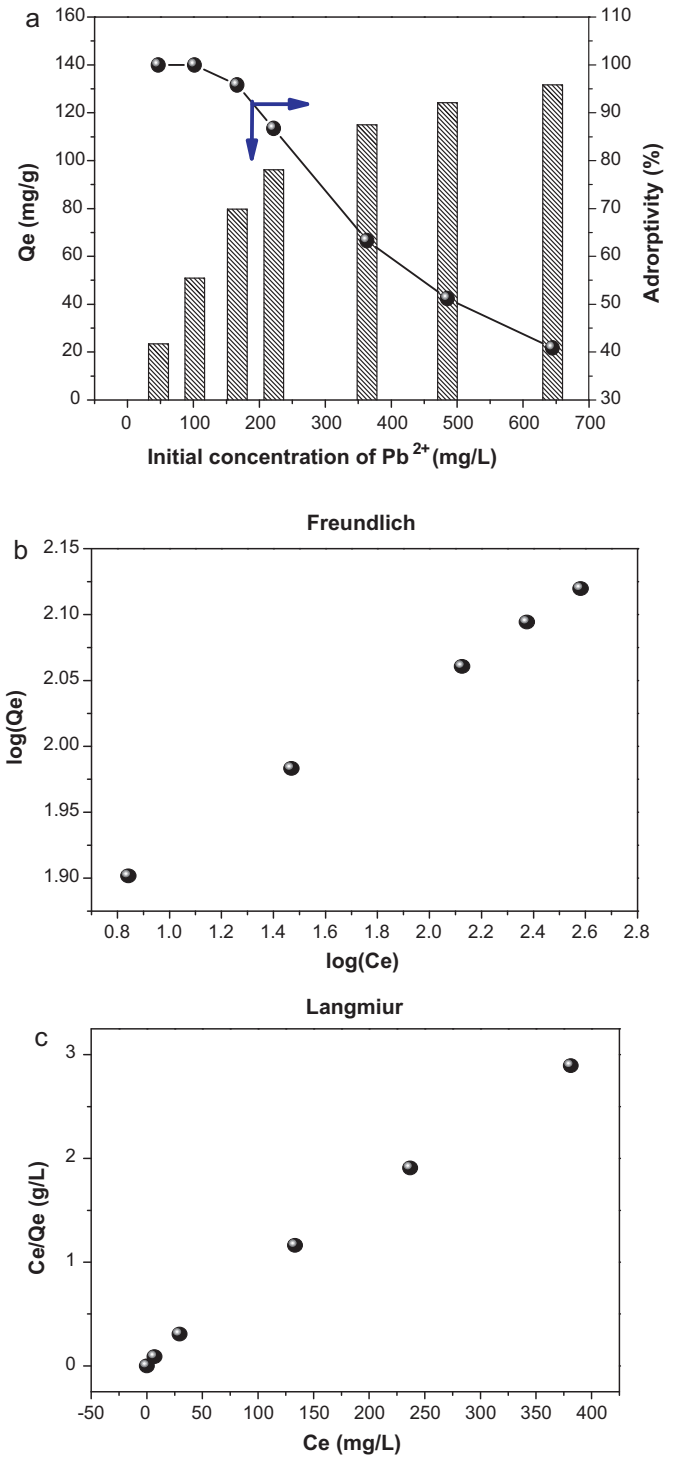

Fig. 9. Adsorption isotherms of ASDO for Pb(II) adsorption: (a) effect of initial concentration on adsorption of ASDO, (b) Freundlich model and (c) Langmuir model.

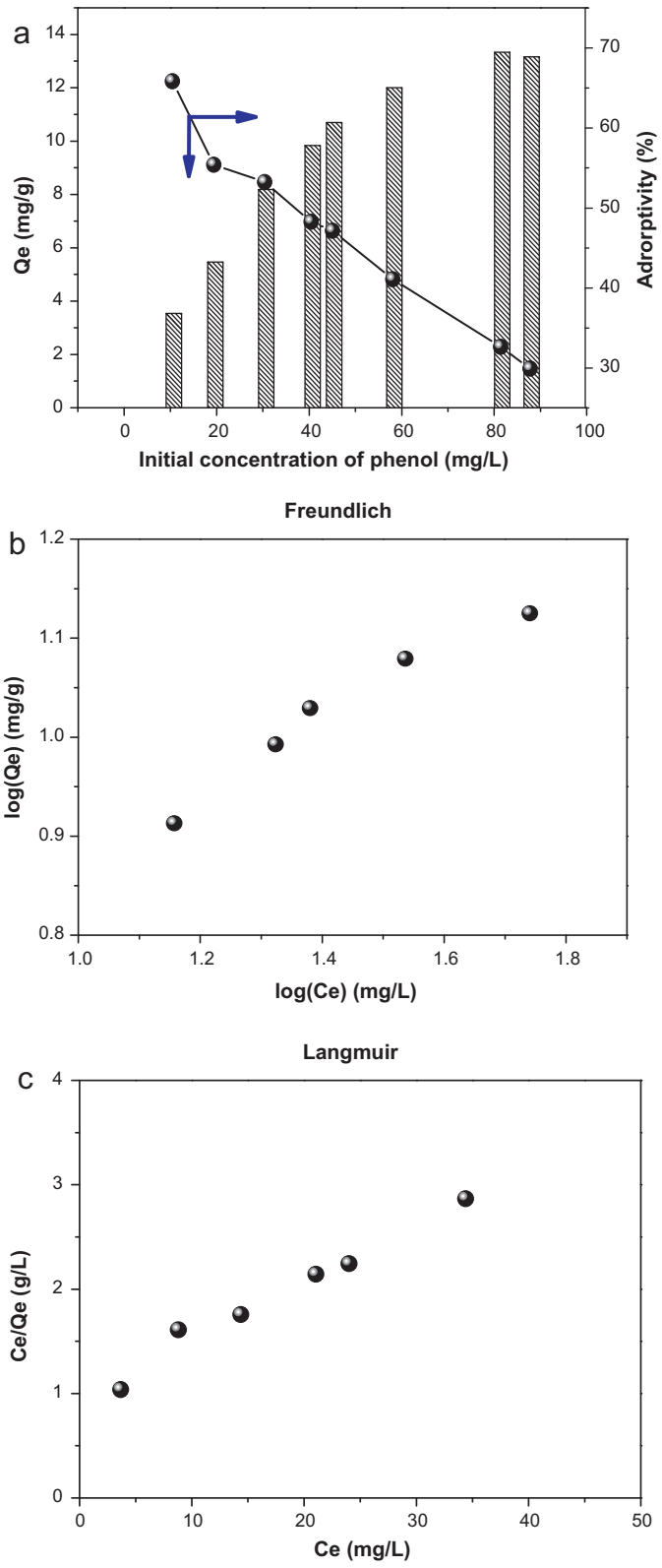

Fig. 10. Adsorption isotherms of ASDO for phenol adsorption: (a) effect of initial concentration on adsorption of ASDO, (b) Freundlich model and (c) Langmuir model.

Pb(II) concentration of around 101.93 mg/l. That is to say, almost all Pb(II) ions will be adsorbed onto the adsorbent if the initial Pb(II) concentration is lower than 101.93 mg/l.

Two mathematical models proposed by Freundlich and Langmuir were used to describe and analyze the sorption isotherm. The sorption data in appropriate concentration range were selected to be modeled, considering that the sorption of Pb(II) and phenol onto ASDO basically reaches equilibrium in 48 h. The modeled quantitative relationship between Pb(II) (or phenol) concentration and the sorption process is shown in Fig. 9b and c (or Fig. 10b and c) and the calculated correlation coefficients and standard deviations are listed in Table 4 (or Table 5). From Table 4 (Table 5), we can conclude as follows: (i) the Langmuir maximum capacity was found to be 131.58 mg/g (18.18 mg/g), but the correlation coefficient R^2 is so low that the calculated results may be not credible. (ii) The

Table 4
Freundlich and Langmuir constants for Pb(II) adsorption on ASDO.

Samples	Langmuir			Freundlich		
	Q_{m1} (mg/g)	K_L (L/mg)	R_1^2	K (mg/g) $(L/mg)^{1/n}$	n	R_2^2
ASDO	131.58	0.1580	0.9972	62.78	8.026	0.9996

Table 5
Freundlich and Langmuir constants for phenol adsorption on ASDO.

Samples	Langmuir			Freundlich		
	Q_{m1} (mg/g)	K_L (L/mg)	R_1^2	K (mg/g) $(L/mg)^{1/n}$	n	R_2^2
ASDO	18.18	0.0574	0.9772	1.581	1.67	0.9920

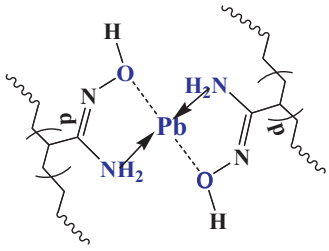

Fig. 11. Scheme of proposed schematic diagram for the complex formation between Pb(II) and ASDO.

slope $1/n$, ranging between 0 and 1 is indicative of the relative energy distribution on the adsorbent surface (or surface heterogeneity) [67]. (iii) The Freundlich correlation coefficient is higher than the Langmuir correlation coefficient. It indicates that the Freundlich isotherm shows better fit to adsorption than the Langmuir isotherm.

3.2.2. Adsorption mechanism

The adsorption mechanism for Pb(II) had been discussed in some reports [68–70] but little study had focus on the adsorption mechanism of phenol [42]. As amidoximes are supposed to be bidentate, two amidoximes may be used for chelate formation with a metal ion, which makes a square planer chelate [71]. Thus, a possible mechanism was presented in Fig. 11.

Phenol adsorption on ASDO is driven by van der Waals interaction between the aromatic ring of phenol molecule and the phenyl ring on the matrix of de-extractant capsules, hydrophobic and hydrogen bonding interaction [42] (as shown in Fig. 12).

3.2.3. The repeating examination of the batch adsorption

Regeneration of the spent adsorbent for repeated reuse is very important in industrial treatment. It was found that the adsorption

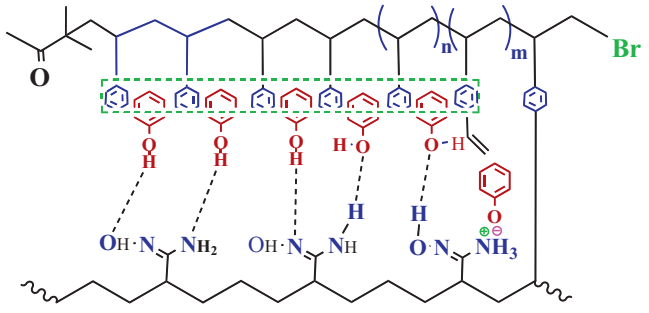

Fig. 12. Scheme of proposed schematic diagram for the adsorption formation between phenol and ASDO.

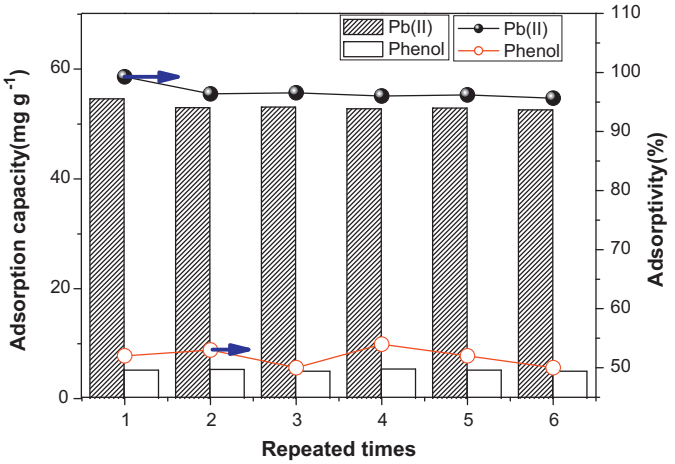

Fig. 13. Repeating adsorption/desorption process with ASDO (C_0Pb(II): 110 mg/l, C_0Phenol: 19.7 mg/l).

behavior of Pb(II) onto ASDO was much dependent on pH value. At high pH value, the hydroxyl bonding interactions between Pb(II) (phenol) and ASDO are weaker or disrupted. Therefore, desorption of the adsorbed tannin from ASDO can take place in alkali solution (1 mol/l NaOH). The adsorption–desorption cycle of ASDO is shown in Fig. 13. It was obvious that ASDO could be utilized repeatedly and the adsorption capacity was slightly declined.

4. Conclusions

In this work, a novel amphiphilic hybrid material was designed and synthesized. FT-IR analysis was used to demonstrate that the synthetic material is the original design goals. We found that the hybrid materials ASDO has excellent adsorption effect of Pb(II) and phenol in the batch adsorption test. The results showed that the maximum adsorption capacity of Pb(II) and phenol onto ASDO was 131.6 mg/g and 18.2 mg/g, respectively. The sorption processes of Pb(II) and phenol onto ASDO includes both chemosorption and physical sorption processes. The sorption all fits the pseudo-second-order kinetics very well with rapid initial sorption rate. The repeating examination revealed that the synthesized hybrid materials maintained high and stable adsorption capacity in the adsorption/desorption experiment for six times.

Acknowledgements

The authors gratefully acknowledge financial supports from the National Major Specific Program of Science and Technology on Controlling and Administering of Water's pollution (2009ZX07212-001-04), Key Research Program of Gansu Province (2GS064-A52-036-02, GS022-A52-082). The authors thank Mrs Sheng and Mr Hu for their supportive help of FT-IR and ICP analyses.

References

[1] P. Bose, M.A. Bose, S. Kumar, Critical evolution of treatment strategies involving adsorption and chelation for wastewater containing copper, zinc and cyanide, Adv. Environ. Res. 7 (2002) 179–195.
[2] M.L. Hassan, N.A. El-Wakil, Heavy metal ion removal by amidoximated bagasse, J. Appl. Polym. Sci. 87 (2003) 666–670.
[3] J. Huang, X. Wang, Q. Jin, Y. Liu, Y. Wang, Removal of phenol from aqueous solution by adsorption onto OTMAC-modified attapulgite, J. Environ. Manage. 84 (2007) 229–236.
[4] N.N. Dutta, S. Brothakur, R. Baruaha, A novel process for recovery of phenol from alkaline wastewater: laboratory study and predesign cost estimate, Water Environ. Res. 70 (1998) 4–9.

[5] A.K. Pinar, O. Güven, Removal of concentrated heavy metal ions from aqueous solutions using polymers with enriched amidoxime groups, J. Appl. Polym. Sci. 93 (2004) 1705–1710.
[6] A. Safa Özcan, G. Özer, Ö. Adnan, Adsorption of lead(II) ions onto 8-hydroxy quinoline-immobilized bentonite, J. Hazard. Mater. 161 (2009) 499–509.
[7] B.E. Reed, S. Arunachalam, Use of granular activated carbon columns for lead removal, J. Environ. Eng. 120 (1994) 416–436.
[8] B.E. Reed, J. Robertson, M. Jamil, Regeneration of granular activated carbon (GAC) columns used for removal of lead, J. Environ. Eng. 121 (1995) 653–662.
[9] S. Akhtar, R. Qadeer, Active carbon as an adsorbent for lead ions, Adsorpt. Sci. Technol. 15 (1997) 815–824.
[10] H. Abdel-Samad, P.R. Watson, An XPS study of the adsorption of lead on goethite (a-FeOOH), Appl. Surf. Sci. 136 (1998) 46–54.
[11] R. Weerasooriya, D. Aluthpatabendi, H.J. Tobschall, Charge distribution multisite complexation (CD-MUSIC) modeling of Pb(II) adsorption on gibbsite, Colloids Surf. A: Physicochem. Eng. Asp. 189 (2001) 131–144.
[12] J.L. Wang, X.M. Zhan, D.C. Ding, D. Zhou, Bioadsorption of lead(II) from aqueous solution by fungal biomass of Aspergillus niger, J. Biotechnol. 87 (2001) 273–277.
[13] W.H. Lo, H.K.H. Chua, A comparative investigation on the biosorption of lead by filamentous fungal biomass, Chemosphere 39 (1999) 2723–2736.
[14] A. Kapoor, T. Viraraghavan, Removal of heavy metals from aqueous solutions using immobilized fungal biomass in continuous mode, Water Res. 32 (1998) 1968–1977.
[15] Y. Liu, W. Wang, A. Wang, Adsorption of lead ions from aqueous solution by using carboxymethyl cellulose-g-poly (acrylic acid)/attapulgite hydrogel composites, Desalination 259 (2010) 258–264.
[16] M.M. Machawe, B.M. Bhekie, Preparation characterization, and application of polypropylene–clinoptilolite composites for the selective adsorption of lead from aqueous media, J. Colloid Interface Sci. 359 (2011) 210–219.
[17] M.P. Papini, A. Bianchi, M. Majone, M. Beccari, Equilibrium modeling of lead adsorption onto a "red soil" as a function of the liquid-phase composition, Ind. Eng. Chem. Res. 41 (2002) 1946–1954.
[18] S.V. Dimitrova, D.R. Mehandgiev, Lead removal from aqueous solutions by granulated blast-furnace slag, Water Res. 32 (1998) 3289–3292.
[19] J.F. Blais, G. Mercier, A. Durand, Lead and zinc recover by adsorption on peat moss during municipal incinerator used lime decontamination, Environ. Technol. 23 (2002) 515–524.
[20] B. Chen, C.W. Hui, G. McKay, Film-pore diffusion modeling for the sorption of metal ions from aqueous effluents onto peat, Water Res. 35 (2001) 3345–3356.
[21] Y.S. Ho, J.C.Y. Nga, G. McKay, Removal of lead(II) from effluents by sorption on peat using second-order kinetics, Sep. Sci. Technol. 36 (2001) 241–261.
[22] C.D. Woolard, K. Petrus, M. van der Horst, The use of a modified fly ash as an adsorbent for lead, Water SA 26 (2000) 531–536.
[23] Q.S. Liu, T. Zheng, P. Wang, Adsorption isotherm kinetic and mechanism studies of some substituted phenols on activated carbon fibers, Chem. Eng. J. 157 (2010) 348–356.
[24] M.H. El-Naas, S. Al-Zuhair, M. Abu-alhaija, Removal of phenol from petroleum refinery wastewater through adsorption on date-pit activated carbon, Chem. Eng. J. 162 (2010) 997–1005.
[25] F.A. Banat, B. Al-Bashir, S. Al-Asheh, O. Hayajneh, Adsorption of phenol by bentonite, Environ. Pollut. 107 (2000) 391–398.
[26] C. Yang, Y. Qian, L.J. Zhang, Solvent extraction process development and onsite trial-plant for phenol removal from industrial coal-gasification wastewater, Chem. Eng. J. 117 (2006) 179–185.
[27] M.T. Reis, O.M. de Freitas, M.R. Ismael, J.M. Carvalho, Recovery of phenol from aqueous solutions using liquid membranes with Cyanex 923, J. Membr. Sci. 305 (2007) 313–324.
[28] C. Bertoncini, J. Raffaelli, L. Fassino, H.S. Odetti, E.J. Bottani, Phenol adsorption on porous and non-porous carbons, Carbon 41 (2003) 1101–1111.
[29] F.Q. An, B.J. Gao, Adsorption of phenol on a novel adsorption material PEI/SiO_2, J. Hazard. Mater. 152 (2008) 1186–1191.
[30] F.Q. An, B.J. Gao, X.Q. Feng, Adsorption mechanism and property of novel composite material PMAA/SiO_2 towards phenol, Chem. Eng. J. 153 (2009) 108–113.
[31] S. Mukherjee, S. Kumar, A. Misra, M. Fan, Removal of phenols from water environment by activated carbon, bagasse ash and wood charcoal, Chem. Eng. J. 129 (2007) 133–142.
[32] K. Nakagawa, A. Namba, S.R. Mukai, H. Tamon, P. Ariyadejwanich, W. Tanthapanichakoon, Adsorption of phenol and reactive dye from aqueous solution on activated carbons derived from solid wastes, Water Res. 38 (2004) 1791–1798.
[33] G. Forland, A. Blokhus, Adsorption of phenol and benzyl alcohol onto surfactant modified silica, J. Colloid Interface Sci. 310 (2007) 431–435.
[34] S. Yapar, M. Yilmar, Removal of phenol by using montmorillonite, clinoptilolite and hydrotalcite, Adsorption 10 (2004) 287–298.
[35] A.E. Navarro, N.A. Cuizano, J.C. Lazo, M.R. Sun-Kou, B.P. Llanos, Comparative study of the removal of phenolic compounds by biological and non-biological adsorbents, J. Hazard. Mater. 164 (2009) 1439–1446.
[36] A.B. Stephen, S.B. Sun, J.F. Lee, N.M. Mortland, Pentachlorophenol sorption by organoclays, Clay Clay Miner. 36 (1988) 125–130.
[37] L.Q. Yang, Y.F. Li, L.Y. Wang, Y. Zhang, X.J. Ma, Z.F. Ye, Preparation and adsorption performance of a novel bipolar PS-EDTA resin in aqueous phase, J. Hazard. Mater. 180 (2010) 98–105.
[38] L.Y. Wang, L.Q. Yang, Y.F. Li, Study on adsorption mechanism of Pb(II) and Cu(II) in aqueous solution using PS-EDTA resin, Chem. Eng. J. 163 (2010) 364–372.
[39] Y. Zhang, Y.F. Li, L.Q. Yang, Characterization and adsorption mechanism of Zn^{2+} removal by PVA/EDTA resin in polluted water, J. Hazard. Mater. 178 (2010) 1046–1054.
[40] X.J. Ma, Y.F. Li, Z.F. Ye, L.Q. Yang, Novel chelating resin with cyanoguanidine group: useful recyclable materials for Hg(II) removal in aqueous environment, J. Hazard. Mater. 185 (2011) 1348–1354.
[41] G.H. Zhao, L.C. Zhou, Y. Li, Enhancement of phenol degradation using immobilized microorganisms and organic modified montmorillonite in a two-phase partitioning bioreactor, J. Hazard. Mater. 169 (2009) 402–410.
[42] G.H. Zhao, Y.F. Li, Preparation of capsules containing 1-nonanol for rapidly removing high concentration phenol from aqueous solution, J. Hazard. Mater. 175 (2010) 715–725.
[43] X.J. Ma, Y.F. Li, Preparation of novel polysulfone capsules containing zirconium phosphate and their properties for Pb(II) removal from aqueous solution, J. Hazard. Mater. 188 (2011) 296–303.
[44] X. Bai, Z.F. Ye, Y.F. Li, Preparation and characterization of a novel macroporous immobilized micro-organism carrier, Biochem. Eng. J. 49 (2010) 264–270.
[45] X. Bai, Z.F. Ye, Y.Z. Qu, Y.F. Li, Immobilization of nanoscale Fe^0 in and on PVA microspheres for nitrobenzene reduction, J. Hazard. Mater. 172 (2009) 1357–1364.
[46] H. Bai, C. Li, G.Q. Shi, Functional composite materials based on chemically converted graphene, Adv. Mater. 23 (2011) 1089–1115.
[47] Y.J. Xu, A. Rosa, X. Liu, D.S. Su, Characterization and use of functionalized carbon nanotubes for the adsorption of heavy metal anions, New Carbon Mater. 26 (2011) 57–62.
[48] P. Xu, H. Tang, S. Li, J. Ren, E. Van Kirk, W.J. Murdoch, M. Radosz, Y. Shen, Enhanced stability of core-surface cross-linked micelles fabricated from amphiphilic brush copolymers, Biomacromolecules 5 (2004) 1736–1744.
[49] J.N. Kizhakkedathu, K.R. Kumar, D. Goodman, D.E. Brooks, Synthesis and characterization of well-defined hydrophilic block copolymer brushes by aqueous ATRP, Polymer 45 (2004) 7471–7489.
[50] K. Matyjaszewski, J. Xia, Atom transfer radical polymerization, Chem. Rev. 101 (2001) 2921–2990.
[51] S.B. Lee, A.J. Russell, K. Matyjaszewski, ATRP synthesis of amphiphilic random, gradient, and block copolymers of 2-(dimethylamino)ethyl methacrylate and n-butyl methacrylate in aqueous media, Biomacromolecules 4 (2003) 1386–1393.
[52] J. Yao, P. Ravi, K.C. Tam, L.H. Gan, Association behavior of poly(methyl methacrylate-b-methacrylic acid-b-methyl methacrylate) in aqueous medium, Polymer 45 (2004) 2781–2791.
[53] M.F. Zhang, T. Breiner, H. Mori, A.H.E. Müller, Amphiphilic cylindrical brushes with poly(acrylic acid) core and poly(n-butyl acrylate) shell and narrow length distribution, Polymer 44 (2003) 1449–1458.
[54] K. Ishizu, J. Satoh, A. Sogabe, Architecture and solution properties of AB-type brush-block-brush amphiphilic copolymers via ATRP techniques, J. Colloid Interface Sci. 274 (2004) 472–479.
[55] B.Z. Zhan, M.A. White, Functionalization of a nano-faujasite zeolite with PEG-grafted PMA tethers using atom transfer radical polymerization, Macromolecules 37 (2004) 2748–2753.
[56] Y.F. Yang, L. Liu, J. Zhang, C.X. Li, H.Y. Zhao, PMMA colloid particles stabilized by layered silicate with PMMA-*b*-PDMAEMA block copolymer brushes and carbon nanotubes, Langmuir 23 (2007) 2867–2873.
[57] W.C. Lin, Q. Fu, Y. Zhang, J.L. Huang, One-pot synthesis of ABC type triblock copolymers via a combination of click chemistry and atom transfer nitroxide radical coupling chemistry, Macromolecules 41 (2008) 4127–4135.
[58] W.X. Wang, Y. Zheng, E. Roberts, C.J. Duxbury, L.F. Ding, D.J. Irvine, S.M. Howdle, Controlling chain growth: a new strategy to hyperbranched materials, Macromolecules 40 (2007) 7184–7194.
[59] S.B. Deng, Y.P. Ting, Characterization of PEI-modified biomass and biosorption of Cu(II), Pb(II) and Ni(II), Water Res. 39 (2005) 2167–2177.
[60] G. Issabayeva, M.K. Aroua, N.M.N. Sulaiman, Removal of lead from aqueous solutions on palm shell activated carbon, Bioresour. Technol. 97 (2006) 2350–2355.
[61] K. Saeed, S. Haider, T.J. Oh, S.-Y. Park, Preparation of amidoxime-modified polyacrylonitrile (PAN-oxime) nanofibers and their applications to metal ions adsorption, J. Membr. Sci. 322 (2008) 400–405.
[62] F. Eloy, R. Lenaers, The chemistry of amidoximes and related compounds, Chem. Rev. 62 (1962) 155–183.
[63] J. Han, R.L. Deming, F. Tao, Theoretical study of hydrogen-bonded complexes of chlorophenols with water or ammonia: correlations and predictions of p*Ka* values, J. Phys. Chem. A 109 (2005) 1159–1167.
[64] K. Haghbeen, L. Raymond, Legge Adsorption of phenolic compounds on some hybrid xerogels, Chem. Eng. J. 150 (2009) 1–7.
[65] X.L. Jin, C. Yu, Y.F. Li, Y.X. Qi, L.Q. Yang, G.H. Zhao, H.Y. Hu, Preparation of novel nano-adsorbent based on organic–inorganic hybrid and their adsorption for heavy metals and organic pollutants presented in water environment, J. Hazard. Mater. 186 (2011) 1672–1680.
[66] Y.J. Zhao, Y. Chen, Adsorption of Hg^{2+} from aqueous solution onto polyacrylamide/attapulgite, J. Hazard. Mater. 171 (2009) 640–646.
[67] W.T. Tsai, Y.M. Chang, C.W. Lai, C.C. Lo, Adsorption of basic dyes in aqueous solution by clay adsorbent from regenerated bleaching earth, Appl. Clay Sci. 29 (2005) 149–154.
[68] Z.J. Yu, E.T. Kang, K.G. Neoh, Amidoximation of the acrylonitrile polymer grafted on poly(tetrafluoroethylene-co-hexafluoropropylene) films and its

relevance to the electroless plating of copper, Langmuir 18 (2002) 10221–10230.
[69] L. Jin, R.B. Bai, Mechanisms of lead adsorption on chitosan/PVA hydrogel beads, Langmuir 18 (2002) 9765–9770.
[70] X. Liu, H. Chen, C.H. Wang, R.J. Qu, C.N. Ji, C.M. Sun, Y. Zhang, Synthesis of porous acrylonitrile/methyl acrylate copolymer beads by suspended emulsion polymerization and their adsorption properties after amidoximation, J. Hazard. Mater. 175 (2010) 1014–1021.
[71] L. Okamoto, T. Sugo, A. Katakai, H. Omichi, Amidocime-group-containing adsorbents for metal ions synthesized by radiation-induced grafting, J. Appl. Polym. Sci. 30 (1985) 2967–2977.